THE JOURNAL OF BIOLOGICAL CHEMISTRY VOL. 288, NO. 18, pp. 13036–13045, May 3, 2013
© 2013 by The American Society for Biochemistry and Molecular Biology, Inc. Published in the U.S.A.

Dentin Phosphoprotein Binds Annexin 2 and Is Involved in Calcium Transport in Rat Kidney Ureteric Bud Cells*[S]

Received for publication, June 7, 2012, and in revised form, March 20, 2013 Published, JBC Papers in Press, March 22, 2013, DOI 10.1074/jbc.M112.389627

Keith Alvares[‡1], **Paula H. Stern**[§], **and Arthur Veis**[‡]

From the Departments of [‡]*Cell and Molecular Biology and* [§]*Molecular Pharmacology and Biological Chemistry, Feinberg School of Medicine, Northwestern University, Chicago, Illinois 60611*

Background: Dentin phosphoprotein (DPP), responsible for tooth mineralization, is also present in nonmineralizing tissues like kidney, lung, and salivary glands.
Results: DPP binds annexin 2 and 6 and plays a role in calcium influx in rat ureteric bud cells.
Conclusion: DPP plays different roles in mineralizing and nonmineralizing tissues.
Significance: This is the first report showing a possible function for DPP in nonmineralizing tissues.

Dentin phosphoprotein (DPP) is the most abundant noncollagenous protein in the dentin, where it plays a major role in the mineralization of dentin. However, we and others have shown that in addition to being present in the dentin, DPP is also present in nonmineralizing tissues like the kidney, lung, and salivary glands, where it conceivably has other functions such as in calcium transport. Because annexins have been implicated as calcium transporters, we examined the relationships between DPP and annexins. In this report, we show that DPP binds to annexin 2 and 6 present in a rat ureteric bud cell line (RUB1). Immunofluorescence studies show that annexin 2 and DPP colocalize in these cells. In addition, DPP and annexin 2 colocalize in the ureteric bud branches of embryonic metanephric kidney. In the RUB1 cells and ureteric bud branches of embryonic kidney, colocalization was restricted to the cell membrane. Studies on calcium influx into RUB cells show that in the presence of anti-DPP, there was a 40% reduction of calcium influx into these cells. We postulate that DPP has different functions in the kidney as compared with the odontoblasts. In the odontoblasts, its primary function is in the extracellular mineralization of dentin, whereas in the kidney it may participate in calcium transport.

Dentin phosphoprotein (DPP),[2] a major noncollagenous protein of dentin, is a highly phosphorylated serine- and aspartic acid-rich protein (1–3). DPP from various species contain 35–45 residue % aspartic acid and 40–55 residue % serine, of which as many as 90% of the serine residues are phosphorylated (4, 5). Because of its high phosphate content, net negative charge, and avid binding to Ca^{2+} ions, DPP has been linked to dentin mineralization (6, 7). Although present in the dentin matrix as an essential macromolecule, DPP is synthesized as a part of a larger precursor protein, dentin sialophosphoprotein (DSPP) (8) that *in vivo* is rapidly processed by scission of a central sequence freeing the amino-terminal domain, dentin sialoprotein, and the carboxyl-terminal domain DPP (9–11), plus a central connecting peptide sequence (12). Dentin sialoprotein and DPP belong to a family of proteins now known as small integrin-binding ligand *N*-linked glycoproteins (SIBLINGs) (13). The SIBLING family includes DSPP, osteopontin, bone sialoprotein, dentin matrix protein 1 (DMP1), and matrix extracellular phosphoglycoprotein (14). They are characterized by common exon-intron features, the presence of the integrin binding tripeptide, Arg-Gly-Asp (RGD), and several conserved phosphorylation and *N*-glycosylation sites (13). The SIBLING genes are clustered together on human chromosome 4 and mouse chromosome 5 (14). Having been first isolated from bone or tooth, expression of the SIBLINGs in adults was generally thought to be limited to mineralizing tissues and to playing a role in mineralization. However, recent reports have shown that various members of this family, such as DMP1, osteopontin, and DPP, are present in other tissues where they conceivably modulate additional biological processes including signaling (15–22). DPP has been implicated to be a coactivator in BMP2 signaling (18) and has also been shown to modulate cell differentiation through integrin signaling and activation of p38, ERK1/2, and JNK, three components of the MAPK pathway (17) and the Smad pathway (23). We have also shown that the developing kidney metanephroi exposed in culture to anti-DMP2 or antisense oligonucleotides have elongated ureteric bud branches but with reduced branching arborization (24). There was also a reduction in the number of glomeruli. Quantitative analysis confirmed that there was a ~50% decrease in the number of glomeruli after the treatment with the anti-DMP2. Also, analysis of a $DSPP^{-/-}$ null mouse at embryonic day 13.5 showed a delayed maturation of the nephron elements and fewer ureteric buds as compared with wild type $DSPP^{+/+}$. Delay in the maturation of the nephrons was reflected by overall smaller size of the metanephros and less polarized epithelial layers in the nephrons (24). Recent studies have shown that kidney development is regulated by the presence of calcium ions (25, 26).

* This work was supported, in whole or in part, by National Institutes of Health Grant DE001374 (to A. V.).
[S] This article contains supplemental Figs. S1 and S2.
[1] To whom correspondence should be addressed: Dept. of Cell and Molecular Biology, Feinberg School of Medicine, Northwestern University, 303 E. Chicago Ave., Chicago, IL 60611. Tel.: 312-503-2628; Fax: 312-503-2544; E-mail: k-alvares@northwestern.edu.
[2] The abbreviations used are: DPP, dentin phosphoprotein; DSPP, dentin sialophosphoprotein; SIBLING, small integrin-binding ligand *N*-linked glycoprotein; DMP, dentin matrix protein; AM, acetyloxymethyl ester.

Because DPP has been implicated in signaling, it was of interest to see whether DPP exerts its function by interacting with another protein. In this report we show that DPP binds annexin 6 and annexin 2 in a rat ureteric bud cell line (RUB1). Furthermore, in these cells and in rat embryonic kidney, DPP and annexin 2 colocalize along the cell membrane. We also show that calcium influx into RUB1 cells was reduced in the presence of anti-DPP antibody.

EXPERIMENTAL PROCEDURES

Expression of DPP in Baculovirus—Based on the known sequences present in the GenBank™, primers were designed to PCR DPP from mouse genomic DNA. The primers used were designed with a BamHI site and an EcoRI site at the 5′ end of the gene-specific sequences (bold letters) to facilitate directional cloning. The mouse DPP cDNA amplified started from the amino acids NSES and included the RGD binding site. This corresponds to amino acid number 469 of the DSPP gene (8). The primers used were 5′-CGCGTGGATCC**AACTCTGAAAGCGCCAATGAGAGTGGC**-3′ (forward) and 5′-CGATGAATTCC**TAATCATCACTGGTTGAGTGGTTAC**-3′ (reverse). Following the PCR, the amplified band was gel-purified, digested with BamHI and EcoRI, and cloned in the baculovirus transfer vector pAcG2T (Pharmingen). This vector expresses the protein as a GST fusion protein. The resulting vector pAcG2T-DPP was then sequenced to verify that DPP was indeed present in frame with the GST protein. The pAcG2T-DPP vector was then cotransfected with BaculoGold linearized baculovirus DNA (Pharmingen) into Sf9 insect cells. 5 days after transfection, the supernatant was serially diluted, and the cells producing the recombinant virus were identified by plaque assay. The virus was then amplified and used to infect fresh Sf9 cells to produce the recombinant protein GST-DPP. The Sf9 cells have the capability to carry out the extensive post-translational phosphorylation, which is the hallmark of DPP. The cells infected with recombinant virus were harvested 3 days postinfection. The cells were then spun down at 2,500 × *g* for 5 min. The cell pellet was resuspended in ice-cold insect cell lysis buffer (Pharmingen) containing reconstituted protease inhibitor mixture at a concentration of 1 ml of lysis buffer per 2×10^7 cells. The cells were lysed on ice for 45 min, and the lysate was cleared of cellular debris by centrifuging at 40,000 × *g* for 45 min. The clear supernatant containing GST-DPP recombinant protein was analyzed on SDS-PAGE gel. The GST-DPP recombinant protein was then purified on a glutathione-Sepharose column (Amersham Biosciences) according to the manufacturer's instructions. The purified DPP was then bound to CNBr-activated Sepharose to generate a DPP-Sepharose affinity column.

Cell Culture—The rat ureteric bud (RUB1) cell line, a gift from Dr. Perantoni (NCI, National Institutes of Health) was grown in DMEM/F-12 medium with 10% fetal bovine serum, 10 ng of TGFα, with 1% antibiotic-antimycotics. After reaching 50% confluence, the cells were then cultured in the original medium or in the presence of 1 mM EDTA for 14 h.

Isolation of DPP-binding Proteins—Crude cell membrane fractions were obtained from rat ureteric bud (RUB1) cell lines using a Mem-PER eukaryotic membrane protein extraction reagent kit (Pierce) according to the manufacturer's instructions. The cells (5×10^6) were centrifuged at 850 × *g* for 2 min, and the pellet was lysed with a proprietary detergent from the kit. A second proprietary detergent was added to solubilize the membrane proteins. The samples were centrifuged at 10,000 × *g* for 3 min at 4 °C. The supernatant was removed, incubated for 10 min at 37 °C, and centrifuged for 2 min at 10,000 × *g* to separate the hydrophobic proteins (bottom layer) from the hydrophilic proteins (top layer) through phase partitioning. The hydrophobic fraction was dialyzed against three changes of binding buffer containing Tris-HCl, pH 7.5, 150 mmol/liter NaCl, 1 mmol/liter $MgCl_2$, 1 mmol/liter $CaCl_2$, and 0.1% sodium deoxycholate for 24 h at 4 °C. Following dialysis, the solubilized membrane fraction was individually incubated with the DPP-Sepharose gel or GST-Sepharose gel (control) overnight with gentle end over end mixing. The next day the resins were poured into columns, and the columns were washed with binding buffer and subsequently eluted with 1-ml aliquots of elution buffer containing Tris-HCl, pH 7.5, 0.1% sodium deoxycholate, 20 mmol/liter EDTA, 20 mmol/liter EGTA, and 150 mmol/liter NaCl. The materials eluted from the DPP affinity and GST columns were concentrated and separated by 12% SDS-polyacrylamide gel electrophoresis under reducing conditions. The gels were either stained with Coomassie Blue or transferred to nitrocellulose membranes. The membranes were incubated with anti-annexin 2 mouse monoclonal antibody (Invitrogen). The primary antibodies were diluted 1:1000. Antibody-reactive material was detected with alkaline phosphatase-conjugated anti-mouse antibody (1:30,000) and visualized by an AP detection kit (Bio-Rad).

Coimmunoprecipitation—The RUB1 cell line was grown in DMEM/F-12 medium as described above. After reaching 80% confluence, the cells were lysed with 50 mM Tris-HCl, pH 7.4, containing 0.1% Nonidet P-40, 0.1% sodium deoxycholate, and 1 mmol/liter $CaCl_2$. This was then centrifuged, and the clarified supernatant was incubated with either anti-annexin 2 or non-specific IgG and rotated at 4 °C overnight. The next day 50 μl of protein A-Sepharose was added to the solution, and incubation was carried on for an additional 2 h at room temperature. The reaction was centrifuged at 10,000 × *g* for 5 min at 4 °C, and the pellet was then washed four times with PBS. After the final wash, the pellet was suspended in 50 μl of Laemmli buffer and separated by 10% SDS-polyacrylamide gel electrophoresis under reducing conditions. The gels were transferred to nitrocellulose membranes. The membranes were incubated overnight with anti-DPP antibody diluted 1:1000. Antibody-reactive material was detected with alkaline phosphatase-conjugated anti-rabbit antibody (1:30,000) and visualized by an AP detection kit (Bio-Rad).

Protein Sequencing Using Mass Spectrometry—SDS-PAGE analysis of the DPP-Sepharose column identified two major protein bands, at ~75 and 40 kDa. There were no bands present in the GST-Sepharose column eluate. Each of these bands isolated from the DPP-Sepharose column were excised from the gel and subjected to in-gel proteolytic digestion with trypsin. The recovered peptides were separated and analyzed using an LTQ mass spectrometer to obtain MS/MS spectra at the Chicago Biomedical Consortium Proteomics facility at University

of Illinois at Chicago. The sequences of the peptides were inferred by matching the MS/MS spectra to protein sequence data bases using the Sequest and Mascot database search engines.

Phosphostaining—Detection of the phosphorylated state of the recombinant GST-DPP was accomplished using Pro-Q Diamond phosphoprotein gel stain, as described by the manufacturer (Molecular Probes; Invitrogen). SDS-PAGE gels were stained with the Pro-Q Diamond phosphoprotein stain and scanned immediately following three washes to reduce background using a Typhoon Trio Imager (Amersham Biosciences). The scanned images were then analyzed by ImageQuant software (version 6.0; Amersham Biosciences).

Immunostaining—For immunostaining, RUB1 cells were grown on chamber slides overnight. Adherent cells were rinsed with PBS, fixed, and permeabilized with methanol at −20 °C for 30 min. The cells were then blocked with 5% BSA and 3% normal goat or donkey antibody in PBS for 4 h at room temperature. Sections of embryonic kidney were deparaffinized and rehydrated through graded alcohol solutions followed by washing with PBS. The cells or sections were then incubated with the anti-DPP (1:200) and anti-annexin 2 (1:200) primary antibody overnight at 4 °C in a humidified chamber. For controls, the primary antibody was omitted. After washing extensively with PBS, the cells and sections were incubated for 1 h at room temperature with the appropriate secondary antibody. All of the secondary antibody incubations were performed in the dark to minimize loss of fluorescent signal caused by photo bleaching. The cells and tissues were then washed extensively in PBS. Immunoreactive areas were visualized using the 100× oil immersion lens of an Olympus series 120Q microscope.

Intracellular Calcium Measurements—The cells were harvested by treatment with 0.1% trypsin, 0.02% EDTA in phosphate buffered saline, washed in DMEM/F-12 medium with 10% fetal bovine serum, and suspended in a loading buffer (145 mM NaCl, 5 mM KCl, 10 mM HEPES, 10 mM glucose, and 1% bovine serum albumin adjusted to pH 7.4). The cells were loaded with 2 μM Fluo-3/AM (Invitrogen) by gentle shaking for 45 min in loading buffer at room temperature. After 45 min, the cells were centrifuged, washed with loading buffer, and resuspended in 22 ml of loading buffer at a concentration of ~5 × 10^5 cells/ml. The cells were divided into three tubes containing ~7 ml each. In tube 1, 50 μl of anti-DPP antibody was added; in tube 2, 50 μl of nonspecific IgG was added. Tube 3, with no addition, served as control. A PerkinElmer Life Sciences LS5 luminescence spectrophotometer was used for fluorometric determination. The excitation wavelength was set at 505 nm, and the emission wavelength was set at 530 nm. For measurement of calcium influx, 2 ml of cell suspension was added to a cuvette and after a 1.5-min base line recording, 10 μl of a 1 mM solution of ionomycin was added to give a final concentration of 5 μM. This was followed by the addition of 4 μl of a 1 M calcium chloride solution at 3.5 min to give a final calcium concentration of 2 mM. The cell suspension in the cuvette was stirred continuously during the experiment. In other experiments, cells preincubated with nonspecific IgG (control) or cells preincubated with anti-DPP were treated with 2 mM calcium, without the prior addition of ionomycin.

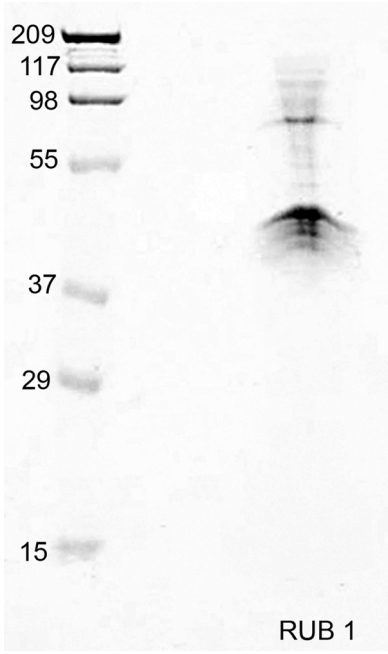

FIGURE 1. **Isolation of two major protein bands from RUB cell solubilized membranes by DPP-Sepharose affinity chromatography.** Results of SDS-PAGE analysis of proteins eluted from the DPP-Sepharose column are shown. Two major bands of ~75 and 40 kDa were isolated. Note that the amount of the 40-kDa band is much greater than the 75-kDa band.

RESULTS

Expression of Phosphorylated DPP in Baculovirus—Supplemental Fig. S1 shows the Stains-All and phosphostaining for baculovirus-expressed (*lanes 2* and *3*) and purified GST-DPP (*lane 4*). DPP expressed in baculovirus shows the characteristic blue-purple metachromatic staining with Stains-All (*lane 4*). Phosphostaining of the purified GST-DPP shows that DPP expressed in baculovirus is phosphorylated (*lane 5*). DPP is a highly acidic protein consisting of many repetitive aspartic acid-serine and aspartic acid-serine-serine motifs, with the majority of the serine residues being phosphorylated *in vivo*.

Identification of Annexin 2 and 6 as DPP-binding Proteins—The phosphorylated GST-DPP isolated from baculovirus was linked to Sepharose to generate a DPP-Sepharose affinity column. To identify DPP-binding proteins, the total membrane protein lysates from RUB cells were incubated with the DPP-Sepharose affinity column in the presence of calcium and magnesium. The columns were then eluted with EDTA and EGTA to isolate the proteins that bound to the column in the presence of calcium and magnesium. The eluted proteins from the column were separated on a SDS-PAGE gel. Fig. 1 shows that two major bands at ~76 and 40 kDa were isolated from the RUB1 cells membrane fraction that was passed over a DPP-Sepharose column. No protein bands were isolated when the same extracts were passed over a GST-Sepharose column, confirming the specificity of the interaction. The ratio of the two proteins 76 kDa:40 kDa was 1:4. There seems to be a greater amount of the 40-kDa band present in the eluate from the RUB cells. These two bands were excised from the gel and subjected to in-gel trypsin digestion and MS/MS analysis. The 75-kDa band was identified as annexin 6 with greater than 95% accuracy by Mascot. The number of peptide matches above identity threshold was 103 with a false discovery rate of 0.97%. The peptides isolated

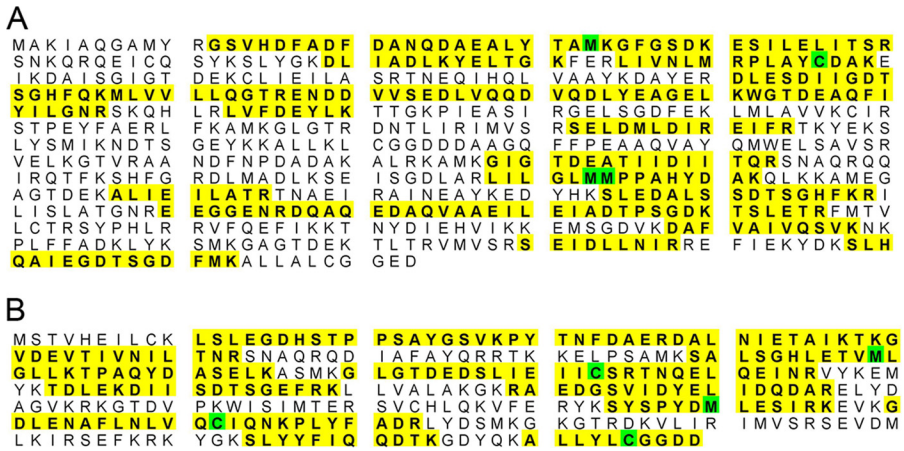

FIGURE 2. **MS/MS analysis identified the two bands to be annexin 2 and 6.** *A*, annexin 6 showing the peptides isolated from the 75-kDa band. The peptides obtained from the 75-kDa band are highlighted in *yellow*. The 75-kDa band was identified as annexin 6 with greater than 95% accuracy by Mascot. The number of peptide matches above the identity threshold was 103, with a false discovery rate of 0.97%. The peptides isolated covered 46% of the protein. *B*, annexin 2 showing the peptides isolated from the 40-kDa band. The peptides obtained from the 40-kDa band are highlighted in *yellow*. The 40-kDa band was identified as annexin 2, with greater than 95% accuracy by Mascot. The number of peptide matches above the identity threshold was 411, with a false discovery rate of 0.49%. The peptides isolated covered 59% of the protein. Residues in green were identified as modified during the process.

covered 46% of the protein. The 40-kDa band was identified as annexin 2 with greater than 95% accuracy by Mascot. The number of peptide matches above identity threshold was 411 with a false discovery rate of 0.49%. The peptides isolated covered 59% of the protein. Fig. 2 shows the peptides isolated (highlighted in *yellow*) for annexin 6 (Fig. 2*A*) and annexin 2 (Fig. 2*B*). The annexin 2 band was four times more intense than the annexin 6 band.

DPP is a calcium-binding protein, and annexin 2 has been identified as a calcium and ion transport protein in kidney (27) and lung airway cells (28), both places where we have shown DPP to be expressed. For these reasons, we decided to concentrate our studies on annexin 2. To confirm that the band isolated from the DPP-Sepharose column was indeed annexin 2, the eluates from the DPP-Sepharose were separated on an SDS-PAGE gel, transferred to nitrocellulose, and subjected to Western blot analysis using anti-annexin 2 (Fig. 3). Western blot analysis confirmed that the 40-kDa protein band bound and eluted from the DPP-Sepharose column was annexin 2. To confirm that annexin 2 and DPP are associated within the cells, we checked whether they would coimmunoprecipitate. Annexin 2 was immunoprecipitated with anti-annexin 2 antibody and protein A-Sepharose. The immunoprecipitate was then run on a 10% polyacrylamide gel and transferred to nitrocellulose membrane and subjected to Western blot analysis using anti-DPP antibody. Western blot analysis confirmed the presence of DPP in the immunoprecipitates brought down by the anti-annexin 2 antibody (Fig. 4). There was one major band seen in the immunoprecipitate with anti-annexin 2 (*lane 3*, *arrow*) that was absent in the immunoprecipitate with nonspecific IgG control (*lane 2*). The two faint lower molecular mass bands also seen in *lane 3* could be degradation products of DPP because they are not seen in the control.

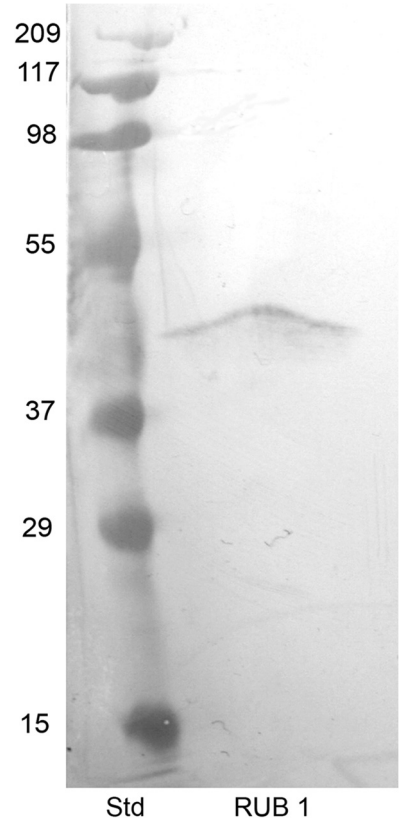

FIGURE 3. **Western blot analysis confirming that the protein eluted from the DPP-Sepharose column is annexin 2.** The proteins eluted from the DPP-Sepharose column were run on a SDS-polyacrylamide gel and transferred to nitrocellulose. The membranes were then probed with annexin 2 antibodies. The *first lane* shows molecular mass standards (*Std*). The *second lane* is solubilized membranes of RUB1 cells bound and eluted from the DPP-Sepharose columns.

Immunofluorescence Analysis of RUB1 Cells—Because DPP binds annexin 2, it was of interest to see whether they colocalize within the cells, using immunofluorescence. The anti-DPP antibody used has been shown by us previously to be specific to DPP and does not react with any other protein in the kidney (24). Immunofluorescence analysis of RUB1 cells with anti-DPP (Fig. 5*C*) and anti-annexin 2 (Fig. 5*B*) antibodies indicate that both are present in the cells. Merging of the two images (Fig. 5*D*) indicates that DPP and annexin 2 colocalized within the cells. In the RUB1 cells (Fig. 5), in addition to the nucleus and the cytosol, DPP showed a punctate staining along the cell

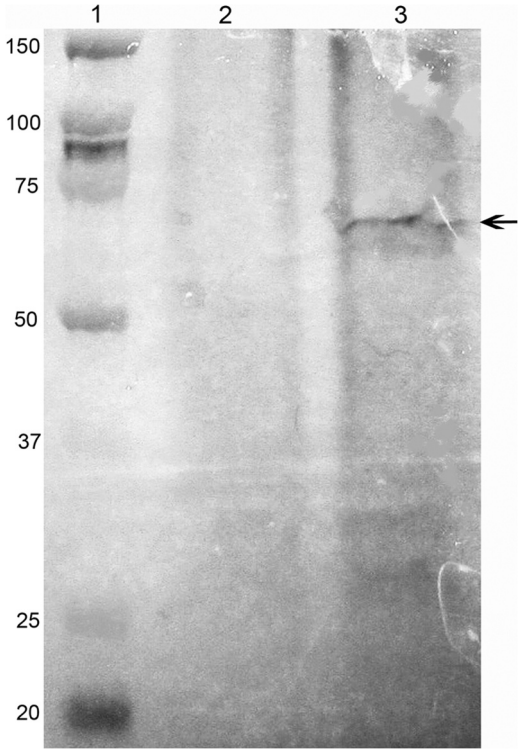

FIGURE 4. **DPP is present in the immunoprecipitate complex brought down by anti-annexin 2 and protein A-Sepharose.** Immunoprecipitates with either nonspecific IgG or anti-annexin 2 were resolved on SDS-PAGE, transferred to nitrocellulose, and probed with anti-DPP. *Lane 1*, molecular mass standards; *lane 2*, the immunoprecipitate brought down with nonspecific IgG; *lane 3*, the immunoprecipitate brought down with anti-annexin 2.

membranes (Fig. 5*C*, *arrows*), where it colocalized with annexin 2 (Fig. 5*D*, *arrows*). Annexin 2 was seen mainly along the cell membranes. DPP could also be seen present in the nucleus (Fig. 5*C*) where annexin 2 is absent. However, in the RUB1 cells, DPP is present along with annexin 2 along the cell membrane, where it could possibly associate with annexin 2 and presumably be involved in calcium transport. Omission of anti-DPP or anti-annexin as controls gave absolutely no immunofluorescence (supplemental Fig. S2). Because the *in vitro* binding of annexin 2 to DPP was calcium-dependent, it was of interest to see whether this was also the case within the cells. Also, the association of annexins with lipid rafts on the membrane has been shown to be calcium-dependent. To test this hypothesis, cells were cultured in the presence of 1 mM EDTA for 14 h. The change in DPP localization was striking when cells were cultured in the presence of 1 mM EDTA (Fig. 6). Under these conditions, there was absolutely no association of DPP with annexin 2. In the presence of 1 mM EDTA, DPP was present exclusively in the nucleus and cytosol with little or no staining in the plasma membrane.

Immunofluorescence Analysis of Embryonic Kidney—Having shown that DPP and annexin 2 are present in the same location in the rat ureteric bud cell (RUB1) lines, the next step was to see whether this also occurs within the developing rat tissues. As reported earlier, DPP was exclusively found in the ureteric bud of the developing kidney (24). Immunofluorescence of embryonic day 14.5 rat embryonic kidney showed the presence of DPP along the developing ureteric bud, (Fig. 7, *A* and *D*), where it colocalized with annexin 2 (Fig. 7, *C* and *F*). In the ureteric bud, as in the RUB1 cells, DPP colocalized with annexin 2 along the cell membrane. In the RUB1 cells, an appreciable amount of DPP could be seen in the cytosol (Fig. 5). However, in the embryonic kidney, DPP was predominantly present as punctate staining along the membrane of the developing ureteric bud (Fig. 7).

Calcium Influx Studies—We investigated the role of DPP on the transport of calcium into RUB1 cells. The cells were suspended in calcium-free flux buffer loaded with Fluo-3/AM and measured for calcium influx as described under "Experimental Procedures." After an initial 1.5-min base-line recording, ionomycin was added to give a final concentration of 5 μM. The addition of ionomycin in the absence of extracellular calcium resulted in a slight increase of $[Ca^{2+}]_i$ followed by a slow decline, suggesting a depletion of intracellular stores. There was no difference between regular cells and cells treated with anti-DPP. At 3.5 min, calcium was added to the cell suspension to give a final concentration of 2 mM. The addition of 2 mM calcium to the suspension resulted in a sustained increase in $[Ca^{2+}]_i$ resulting from an influx of calcium into the cells. This increase eventually plateaued. Responses of cells treated with nonspecific IgG were no different from those of control untreated cells in two separate experiments (Fig. 8*A*). The increase in calcium was lower in cells that were pretreated with anti-DPP (Fig. 8*B*). This difference between untreated cells and cells treated with anti-DPP was consistently observed in four separate experiments. Table 1 shows the fluorescence values for control and anti-DPP-treated cells. The mean fluorescence value for control cells was 13.3 ± 0.42 ($n = 4$), whereas that for cells treated with antibody was 8.1 ± 0.58. ($n = 4$). Inclusion of anti-DPP antibody resulted in a 40% reduction in the amount of calcium influx into the cells.

We next decided to see whether the RUB1 cells were capable of taking up calcium in the absence of ionophore stimulation. To do this, RUB1 cells, in two separate experiments, were pretreated with either nonspecific IgG or anti-DPP antibody and then treated with 2 mM calcium without ionomycin treatment. As seen in Fig. 9, treatment with 2 mM calcium resulted in a slow but steady rise in intracellular calcium, which was once again reduced when the cells were treated with anti-DPP antibody.

DISCUSSION

DPP was first identified in the tooth, where it has been shown to play a role in the mineralization of dentin because of its ability to bind to calcium (1, 29–31). Subsequently, we and others have shown DPP to be present in other nonmineralizing tissues, in which they may conceivably modulate other biological processes (19–21, 24). We have previously shown that in addition to the odontoblasts in developing incisors, DPP is also found in the ureteric bud branches of embryonic metanephric kidney, alveolar epithelial buds of the developing lung, and hair follicles (24). DPP has also been shown to have a signaling role, signaling through the MAP kinase (17) and Smad kinase pathways (23) possibly by interaction with integrins. In an attempt to elucidate its role in nonmineralizing tissues, we searched for DPP-binding proteins in a rat ureteric bud cell line (RUB1). In this report, we show that DPP binds to annexin 2 and annexin 6

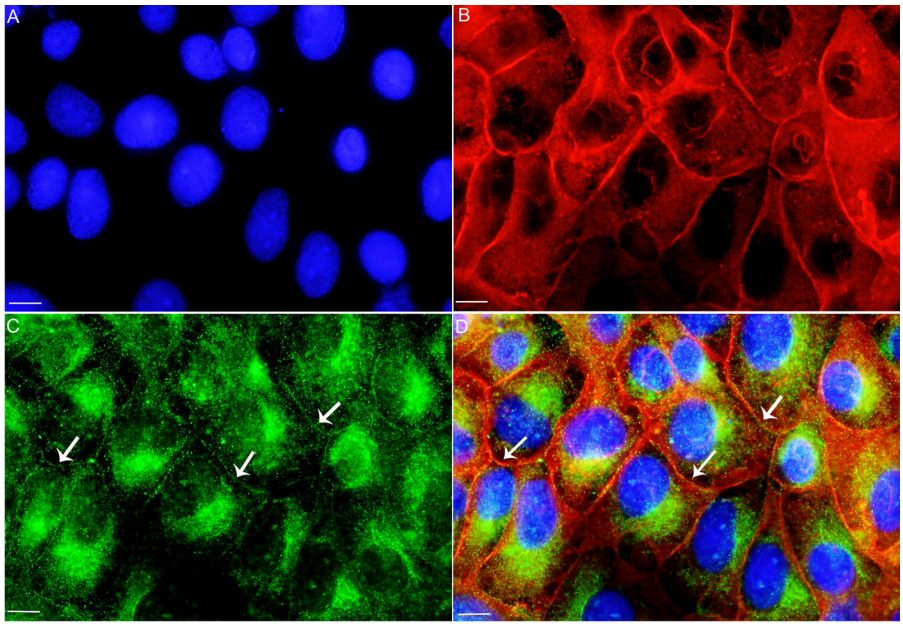

FIGURE 5. **Annexin 2 and DPP colocalize on the cell membrane.** Immunofluorescence of rat ureteric bud cells is shown. *A*, DAPI staining to visualize the nucleus. *B* and *C*, RUB1 cells were grown on chamber slides, fixed, permeabilized, and reacted with anti-annexin 2 (*B*) and anti-DPP (*C*) antibodies. *D*, merging the DAPI, annexin 2, and DPP images indicates that DPP and annexin 2 colocalized at the cell plasma membrane. The *arrows* in *C* and *D* show the plasma membrane. Omission of primary antibody in the reaction gave no immunofluorescence signals. *Bar*, 10 μm.

in this cell line. Upon gel electrophoresis of the proteins binding to DPP from the RUB cell extract, the annexin 2 band was four times greater in intensity than the annexin 6. This could reflect either a greater affinity or a greater amount of annexin 2 in this cell line. The binding of annexins to DPP was specific, because a column of GST-Sepharose failed to isolate any annexins. It is possible that the high concentration of DPP on the column was responsible for DPP displacing the other binding partners of annexin 2. Annexin 2 has been shown to form complexes with other proteins (27, 28, 32–36). As seen in Fig. 2, there are other minor bands present in the elution. These minor bands could be either other proteins bound to DPP or proteins bound to annexin 2. Our current data do not allow us to differentiate between these two possibilities. DPP could be bound to annexin 2 alone or could be a part of a complex. We do not propose that all the annexin 2 present in the cell is bound to DPP because, as mentioned above, annexin 2 has been shown to have a number of other binding partners. Also not all the DPP present in the cell is bound to annexin 2. In the RUB1 cell line, DPP was present in the nucleus, in the cytosol, and also along the cell membrane. DPP has also been shown by others to be present in the cytosol and also in the nucleus in odontoblastic cell lines (37, 38). We now show that in addition to the cytosol and the nucleus, DPP is also present along the cell membrane in RUB1 cells. Annexin 2 was localized in these cells in the cytosol and along the cell membrane where it colocalized with DPP. DPP is present in the nucleus, where annexin 2 is absent (Figs. 6 and 7), and in the cytosol where it most likely is not bound to annexin. It is only the DPP present along the cell membrane that associates with annexin 2. We believe that the interaction between DPP and annexin 2 occurs on the cell membrane and not the extracellular matrix because annexin 2 is not an extracellular matrix protein and is present mainly on the membranes. Further, because we have shown that DPP is involved in calcium uptake and this uptake was inhibited by the addition of anti-DPP, the calcium-binding sites of DPP should be exposed on the outside of the plasma membrane. Interestingly, the anti-DPP antibody showed a punctate staining along the cell membrane, whereas annexin 2 was uniform along the membrane. This might reflect the greater amount of annexin 2 along the membrane and our proposal that not all annexin 2 is bound to DPP. Because DPP does not contain a membrane-spanning region, we propose that the presence of DPP along the cell membrane is due to its association with annexin 2. The binding of DPP to annexin 2 is physiological, because immunoprecipitation of annexin 2 also brings down DPP in the complex.

DPP and annexin 2 were also colocalized in the ureteric bud branches of embryonic metanephric kidney. In the ureteric bud of the metanephric kidney and the RUB1 cell line, the colocalization was seen along the cell membrane. Annexins 2, 5, and 6 form calcium channels in the plasma membrane of terminally differentiated growth plate chondrocytes and mediate calcium influx into these cells (39). Annexin 2 has been described as a cell surface receptor for extracellular matrix molecules such as tenascin-C and proteolytic enzymes including tissue plasminogen activator and cathepsin B (40–42). DPP is a highly acidic protein and does not have any membrane-spanning regions. Therefore its association with the membranes in the rat ureteric bud branches and the RUB cell line is probably through interaction with another protein. In this report, we have shown that the presence of DPP along the plasma membrane may be by virtue of its binding to annexin 2. The binding of DPP to annexin 2 was calcium-dependent. In the *in vitro* studies, annexin 2 was bound to DPP in the presence of calcium and then eluted from the column in the presence of EDTA and EGTA. In the cell culture studies, culturing the cells for 14 h in the presence of EDTA completely abolished the binding of DPP to annexin 2. DPP was then no longer associated with the mem-

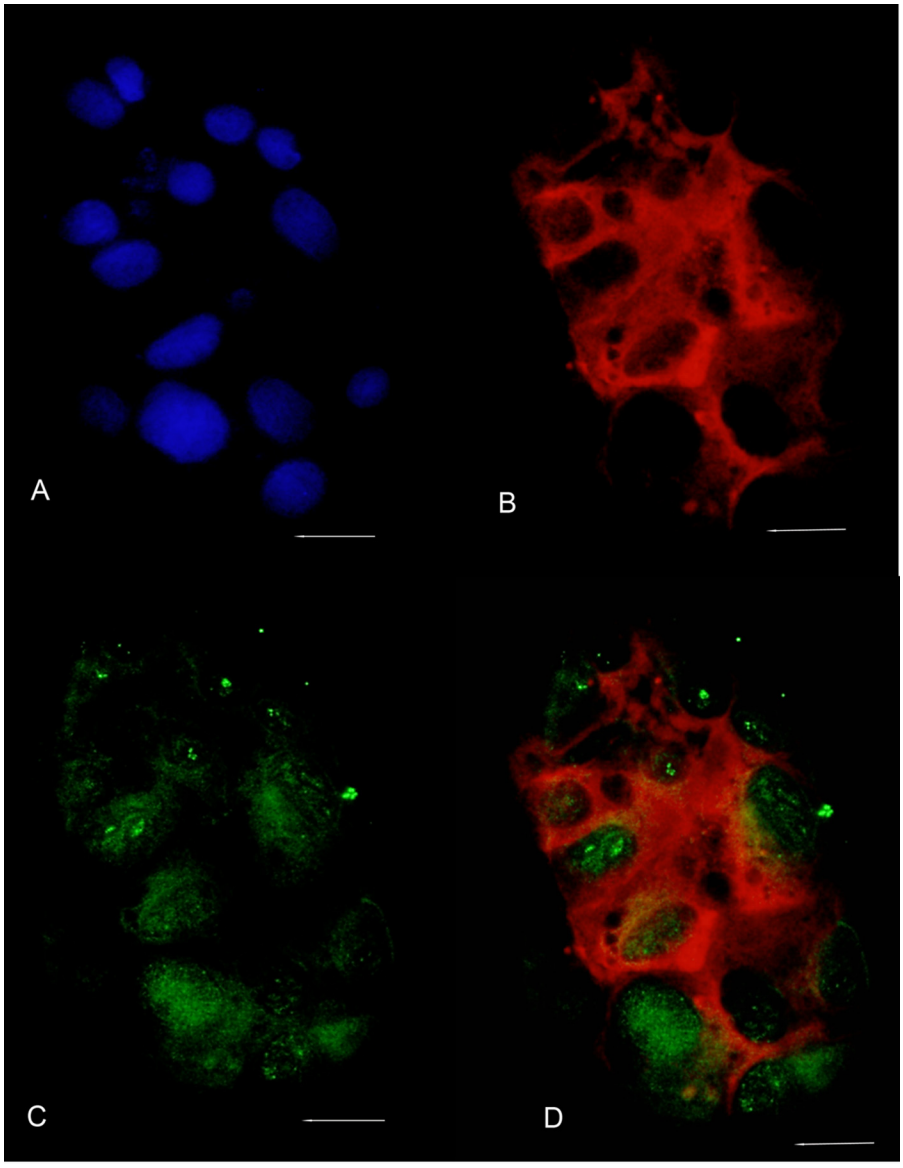

FIGURE 6. **Culturing cells in the presence of EDTA disrupts colocalization of annexin 2 and DPP.** Immunofluorescence rat ureteric bud cells grown in the presence of 1 mM EDTA is shown. *A*, DAPI staining to visualize the nuclei. *B* and *C*, RUB1 cells were grown on chamber slides in the presence of 1 mM EDTA, fixed, permeabilized, and reacted with anti-annexin 2 (*B*) and anti-DPP (*C*) antibodies. *D*, merging the annexin 2 and DPP images indicates that there is no colocalization between DPP and annexin 2 at the cell plasma membrane. *Bar*, 100 μm.

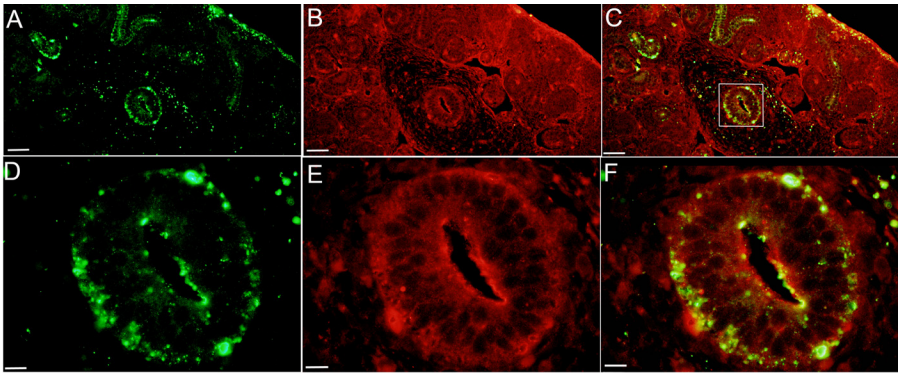

FIGURE 7. **Annexin 2 and DPP colocalized in 14.5-day embryonic kidney.** Immunofluorescence of 14.5-day rat embryonic kidney is shown. The area shown contains the developing ureteric bud. *A* and *D* are stained with anti-DPP. *B* and *E* are stained with anti-annexin 2. *C* and *F* are overlays of the two. In *A–C*, the the *scale bars* indicate 50 μm. *D–F* are 5-fold higher magnifications of the *boxed area* in *C*, and the *scale bars* indicate 10 μm.

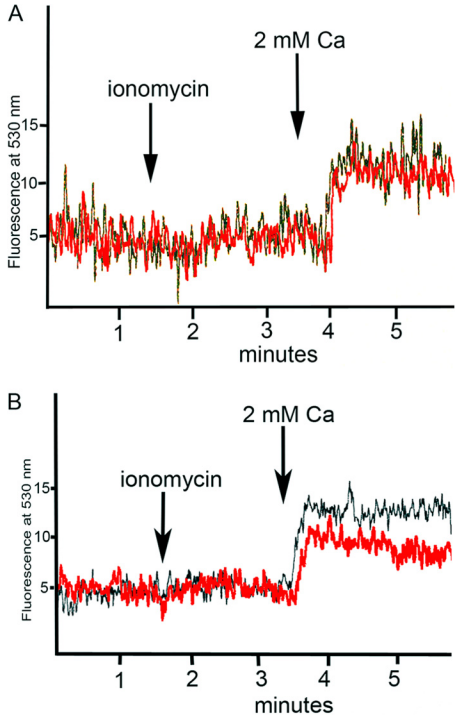

FIGURE 8. **Incubation of cells with anti-DPP lowers calcium uptake.** Calcium uptake in RUB1 cells is shown. $[Ca^{2+}]_i$ was measured as described under "Experimental Procedures." RUB1 cells were loaded with Fluo-3/AM, washed, and suspended in calcium- and magnesium-free flux buffer and then stimulated with 5 μM ionomycin and 2 mM calcium at the time points indicated. *A* shows calcium influx by cells alone (*black trace*) and cells treated with nonspecific IgG (*red trace*). *B* shows calcium influx by cells alone (*black trace*) and cells treated with anti-DPP (*red trace*).

TABLE 1

Fluorescence values for control and anti-DPP-treated cells

Maximum fluorescence obtained when cells loaded with 2 μM Fluo-3/AM were treated with 5 μM ionomycin followed by 2 mM calcium. The cells were suspended in calcium-free flux buffer and loaded with Fluo-3/AM as described under "Experimental Procedures." They were either used as such (control cells) or treated with anti-DPP antibody. In experiment 4, control cells were treated with nonspecific IgG. The table shows the maximum fluorescence values obtained after the addition of 5 μM ionomycin followed by the addition 2 mM calcium chloride.

	Relative fluorescence	
Independent replicates	Control cells	Anti-DPP-treated cells
Experiment 1	14	7.7
Experiment 2	13.2	8.1
Experiment 3	13.1	9
Experiment 4	12.9	7.5
Mean	13.3	8.1
Standard deviation	0.4	0.6

brane and could be seen predominantly in the cytoplasm and nucleus of these cells. Thus, the localization of DPP in the RUB1 cells appears to be dependent on the calcium environment.

Interestingly, like DPP, the annexins have also been shown to bind to calcium. Calcium is recognized as an important regulatory element for many cellular processes. An increase in the cytosolic calcium concentration, which occurs in many cell types after stimulation by hormones, controls a diverse range of cell functions including adhesion, motility, gene expression, and proliferation. Calcium ions have also been shown to play a role in kidney development (25, 26).

Several studies have implicated annexins in complex with S100 proteins in the regulation of trafficking and function of several ion channels. The annexin 2-S100A10 complex binds

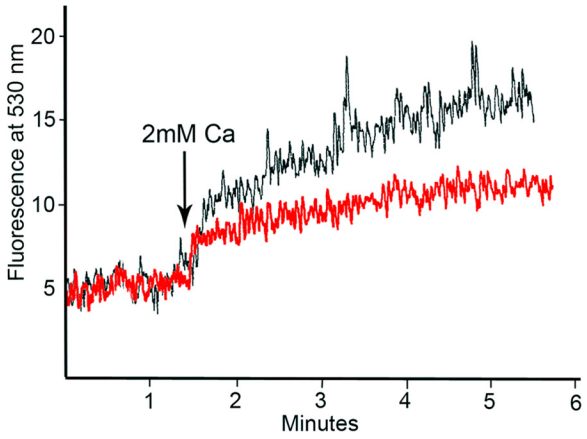

FIGURE 9. **Calcium uptake in the absence of ionophore stimulation.** Calcium uptake in RUB1 cells is shown. $[Ca^{2+}]_i$ was measured as described under "Experimental Procedures." RUB1 cells were loaded with Fluo-3/AM, washed, and suspended in calcium- and magnesium-free flux buffer and then stimulated with 2 mM calcium at 1.5 min. The *black trace* shows calcium influx by cells treated with nonspecific IgG, whereas the *red trace* shows calcium influx by cells treated with anti-DPP.

directly to several plasma membrane ion channels, and this correlates with their incorporation into the plasma membrane. The tetrodotoxin-resistant sodium channel Nav 1.8 and the 2P domain potassium channel TASK-1 form complexes with annexin 2 (44, 45). In addition, the annexin 2-S100A10 complex also interacts with the epithelial calcium channels TRPV5 and TRPV6. The functions of these channels are dependent on their interaction with the annexin 2-S100A10 complex (27).

Transient receptor potential channels TRPV5 and TRPV6 have an important function in Ca^{2+} uptake by kidney (27). These channels are constitutively active at low intracellular Ca^{2+} and physiological membrane potential and have a high selectivity for Ca^{2+}. They are regulated by associated proteins, including calmodulin, 80K-H, Rab11a, $Na^+/H+$ exchanger regulatory factor 2, and the annexin A2-S100A10 complex (46). Also annexins 2, 5, and 6 form calcium channels in the plasma membrane of terminally differentiated growth plate chondrocytes and mediate calcium influx into these cells (39). Annexins 2, 5, and 6 are major components of matrix vesicles that mineralize, whereas they are absent in vesicles that do not mineralize (47). Also, it has been demonstrated that these annexins form calcium channels in matrix vesicles, enabling the influx of calcium (47).

Because annexin 2 has been shown to bind as a complex to calcium transporters and DPP is a calcium-binding protein, this led us to examine whether DPP might be another protein associated with the annexin 2 complex and play a role in Ca^{2+} transport in these nonmineralizing tissues. After depletion of intracellular stores of calcium, the addition of 2 mM calcium led to a sustained rise in intracellular calcium, which eventually plateaued. The rise in intracellular calcium was lower when the cells were preincubated with anti-DPP antibodies. The rise in intracellular calcium was indistinguishable from control cells when preincubated with nonspecific IgG. Preincubation of the cells (with or without ionomycin treatment) with anti-DPP antibody resulted in a 40 ± 5% reduction in calcium influx, which was consistently observed in six different experiments, proving that DPP does play a role in calcium transport in the

kidney. The rise in intracellular calcium, although not completely inhibited, was always lower when cells were treated with the anti-DPP antibody. This lack of total inhibition is expected because DPP would be only one of the many calcium channels present on the cell membrane. Treatment of cells with ionomycin prior to the addition of calcium resulted in a jump in intracellular calcium, which eventually plateaued. However, when cells were treated with calcium in the absence of ionomycin treatment, there was a slow steady rise in intracellular calcium. One explanation for this difference could be that ionomycin depletes intracellular calcium stores, resulting in the opening of all the calcium channels to give a rapid rise in calcium influx. However, in both cases, with or without ionomycin treatment, preincubation with anti-DPP resulted in an inhibition of calcium uptake.

We have previously shown that inclusion of anti-DPP antibodies in organ culture of metanephroi harvested from embryonic day 13.5 mice resulted in a decrease in the ureteric bud iterations and a marked dysmorphogenesis of their branches (24). This is pertinent in light of recent reports that kidney development is controlled by calcium ions (25, 26). The failure to completely abolish the rise in intracellular calcium could also explain the differences seen in organ culture of the metanephroi and the $DSPP^{-/-}$ knock-out mouse. In the more stressful and acute condition of the organ culture, we see dysmorphogenesis of the kidney, whereas in the $DSPP^{-/-}$ knock-out mouse we see only a retardation in kidney maturation (24). In the $DSPP^{-/-}$ knock-out mouse, presumably other calcium channels compensate for the lack of DPP, leading to only a retardation in maturation. Finally, it is worth pointing out that in the adult kidney, DPP is present in the proximal and distal convoluted tubule (20, 22), both sites known to be involved in calcium transport (48).

In conclusion, we have shown that DPP associates with annexin 2 on the cell membrane in the ureteric bud branches of embryonic metanephric kidney and the RUB1 cell line. In the RUB1 cell line, DPP also plays a role in calcium influx. In the odontoblasts, DPP functions in the mineralization of dentin. However, in nonmineralizing tissues like the kidney, DPP may play a role in the transport of calcium. Based on the observations reported here, we conclude that DPP has different functions in different tissues and, depending upon the local circumstances, is processed differently in its route to the cell surface and extracellular matrix.

Acknowledgments—We thank Dr. A. Perantoni (NCI, National Institutes of Health) for the rat ureteric bud cells and Dr. Y. S. Kanwar (Northwestern University) for sections of embryonic rat metanephric kidneys.

REFERENCES

1. Lee, S. L., Veis, A., and Glonek, T. (1977) Dentin phosphoprotein. An extracellular calcium binding protein. *Biochemistry* **16,** 2971–2979
2. Dimuzio, M. T., and Veis, A. (1978) The biosynthesis of phosphophoryns and dentin collagen in the continuously erupting rat incisor. *J. Biol. Chem.* **253,** 6845–6852
3. Dimuzio, M. T., and Veis, A. (1978) Phosphophoryns. Major noncollagenous proteins of the rat incisor dentin *Calcif. Tissue Res*. **25,** 169–178
4. Stetler-Stevenson, W. G., and Veis, A. (1983) Bovine dentin phosphophoryn. Composition and molecular weight. *Biochemistry* **22,** 4326–4335
5. Rahima, M., and Veis, A. (1988) Two classes of dentin phosphophoryns, from a wide range of species, contain immunologically cross-reactive epitope regions. *Calcif. Tissue Res.* **42,** 104–112
6. Veis, A., and Sabsay, B. (1982) Bone and tooth formation. Insights into mineralization stratergies. In *Biomineralization and Biological Metal Accumulation* (P. Westbroek and E.W. deJong, eds) pp. 273–284, D. Reidel Pub. Co., Dordrecht, The Netherlands
7. Veis, A. (1988) Phosphoproteins from teeth and bone. *CIBA Found. Symp.* **136,** 161–177
8. Feng, J. Q., Luan, X., Wallace, J., Jing, D., Ohshima, T., Kulkarni, A. B., D'Souza, R. N., Kozak, C. A., and MacDougall, M. (1998) Genomic organization, chromosomal mapping, and promoter analysis of the mouse dentin sialophosphoprotein (DSPP) gene, which codes for both dentin sialoprotein and dentin phosphoprotein. *J. Biol. Chem.* **273,** 9457–9464
9. George, A., Srinivasan, R., Thotakura, S. R., Liu, K., and Veis A. (1999) Rat dentin matrix protein 3 is a compound protein of rat dentin sialoprotein and phosphophoryn. *Connect. Tissue Res.* **40,** 49–57
10. Gu, K., Chang, S., Ritchie, H. H., Clarkson, B. H., and Rutherford, R. B. (2000) Molecular cloning of a human dentin sialophosphoprotein gene. *Eur. J. Oral Sci.* **108,** 35–42
11. Ritchie, H. H., and Wang, L. (2000) The presence of multiple rat DSP-PP transcripts. *Biochim. Biophys. Acta* **1493,** 27–32
12. Butler, W. T., Brunn, J. C., Qin, C., and McKee, M. D. (2002) Extracellular matrix proteins and dynamics of dentin formation. *Connect. Tissue Res*. **43,** 301–307
13. Fisher, L. W., Torchia, D. A., Fohr, B., Young, M. F., and Fedarko, N. S. (2001) Flexible structures of SIBLING proteins, bone sialoprotein, and osteopontin. *Biochem. Biophys. Res. Commun.* **280,** 460–465
14. Fisher, L. W., and Fedarko, N. S. (2003) Six genes expressed in bones and teeth encode the current members of the SIBLING family of proteins. *Connect. Tissue Res.* **44,** 33–40
15. Jain, A., Karadag, A., Fohr, B., Fisher, L. W., and Fedarko, N. S. (2002) Three SIBLINGs (small integrin-binding ligand, *N*-linked glycoproteins) enhance factor H's cofactor activity enabling MCP-like cellular evasion of complement-mediated attack. *J. Biol. Chem.* **277,** 13700–13708
16. Riminucci, M., Corsi, A., Peris, K., Fisher, L. W., Chimenti, S., and Bianco, P. (2003) Coexpression of bone sialoprotein (BSP) and the pivotal transcriptional regulator of osteogenesis, Cbfa1/Runx2, in malignant melanoma. *Calcif Tissue Int.* **73,** 281–289
17. Jadlowiec, J., Koch, H., Zhang, X., Campbell, P. G., Seyedain, M., and Sfeir, C. (2004) Phosphophoryn regulates the gene expression and differentiation of NIH3T3, MC3T3-E1, and human mesenchymal stem cells via the integrin/MAPK signaling pathway. *J. Biol. Chem.* **279,** 53323–53330
18. Saito, T., Kobayashi, F., Fujii, T., and Bessho, K. (2004) Effect of phosphophoryn on rhBMP-2-induced bone formation. *Arch. Oral Biol,* **49,** 239–243
19. Fedarko, N. S., Jain, A., Karadag, A., and Fisher, L. W. (2004) Three small integrin binding ligand N-linked glycoproteins (SIBLINGs) bind and activate specific Matrix Metalloproteinases. *FASEB J.* **18,** 734–736
20. Ogbureke, K. U., and Fisher, L. W. (2005) Renal expression of SIBLING proteins and their partner matrix metalloproteinases (MMPs). *Kidney Int.* **68,** 155–166
21. Chaplet, M., Waltregny, D., Detry, C., Fisher, L. W., Castronovo, V., and Bellahcène, A. (2006) Expression of dentin sialophosphoprotein in human prostate cancer and its correlation with tumor aggressiveness. *Int. J. Cancer.* **118,** 850–856
22. Prasad, M., Zhu, Q., Sun, Y., Wang, X., Kulkarni, A., Boskey, A., Feng, J. Q., and Qin, C. (2011) Expression of dentin sialophosphoprotein in non-mineralized tissues. *J. Histochem. Cytochem.* **59,** 1009–1021
23. Jadlowiec, J. A., Zhang, X., Li, J., Campbell, P. G., and Sfeir, C. (2006) ECM-mediated signaling by dentin phosphophoryn involves activation of the Smad pathway independent of BMP. *J. Biol. Chem.* **281,** 5341–5347
24. Alvares, K., Kanwar, Y. S., and Veis, A. (2006) Expression and potential role of dentin phosphophoryn (DPP) in mouse embryonic tissues involved in epithelial-mesenchymal interactions and branching morphogenesis. *Dev. Dyn.* **235,** 2980–2990

25. Burn, S. F., Webb, A., Berry, R. L., Davies, J. A., Ferrer-Vaquer, A., Hadjantonakis, A. K., Hastie, N. D., and Hohenstein, P. (2011) Calcium/NFAT signaling promotes early nephrogenesis. *Dev. Biol.* **352,** 288–298
26. Gilbert, T., Leclerc, C., and Moreau, M. (2011) Control of kidney development by calcium ions. *Biochimie* **93,** 2126–2131
27. van de Graaf, S. F., Hoenderop, J. G., Gkika, D., Lamers, D., Prenen, J., Rescher, U., Gerke, V., Staub, O., Nilius, B., and Bindels, R. J. (2003) Functional expression of the epithelial Calcium channels (TRPV5 and TRPV6) requires association of the S100A10-annexin 2 complex. *EMBO J.* **22,** 1478–1487
28. Borthwick, L. A., Neal, A., Hobson, L., Gerke, V., Robson, L., and Muimo, R. (2008) The annexin 2-S100A10 complex and its association with TRPV6 is regulated by cAMP/PKA/CnA in airway and gut epithelia. *Cell Calcium* **44,** 147–157
29. Veis, A., and Perry, A. (1967) The phosphoprotein of the dentin matrix. *Biochemistry* **6,** 2409–2416
30. Zanetti, M., de Bernard, B., Jontell, M., and Linde, A. (1981) Ca^{2+}-binding studies of the phosphoprotein from rat-incisor dentine. *Eur. J. Biochem.* **113,** 541–545
31. MacDougall, M., Zeichner-David, M., and Slavkin, H. C. (1985) Production and characterization of antibodies against murine dentine phosphoprotein. *Biochem. J.* **232,** 493–500
32. Lewit-Bentley, A., Réty, S., Sopkova-de Oliveira Santos, J., and Gerke, V. (2000) S100-annexin complexes. Some insights from structural studies. *Cell Biol. Int.* **24,** 799–802
33. Réty, S., Sopkova, J., Renouard, M., Osterloh, D., Gerke, V., Tabaries, S., Russo-Marie, F., and Lewit-Bentley, A. (1999) The crystal structure of a complex of p11 with the annexin II N-terminal peptide. *Nat. Struct. Biol.* **6,** 89–95
34. Thiel, C., Osborn, M., and Gerke, V. (1992) The tight association of the tyrosine kinase substrate annexin II with the submembranous cytoskeleton depends on intact p11- and Ca21-binding sites. *J. Cell Sci.* **103,** 733–742
35. Zeng, F.-Y., Gerke, V., and Gabius, H.-J. (1993) Identification of annexin II, annexin VI and glyceraldehyde-3-phosphate dehydrogenase as calcyclin-bindingproteins in bovine heart. *Int. J. Biochem.* **25,** 1019–1027
36. Ma, K., Simantov, R., Zhang, J.-C., Silverstein, R., Hajjar, K. A., and McCrae, K. R. (2000) High affinity binding of β_2-glycoprotein I to human endothelial cells is mediated by annexin II. *J. Biol. Chem.* **275,** 15541–15548
37. Hao, J., Ramachandran, A., and George, A. (2009) Temporal and spatial localization of the dentin matrix proteins during dentin diomineralization. *J. Histochem. Cytochem.* **57**, 227–237
38. Chen, S., Gluhak-Heinrich, J., Martinez, M., Li, T., Wu, Y., Chuang, H. H., Chen, L., Dong, J., Gay, I., and MacDougall, M. (2008) Bone morphogenetic protein 2 mediates dentin sialophosphoprotein expression and odontoblast differentiation via NF-Y signaling. *J. Biol. Chem.* **283,** 19359–19370
39. Wang, W., and Kirsch, T. (2002) Retinoic acid stimulates annexin-mediated growth plate chondrocyte mineralization. *J. Cell Biol.* **157,** 1061–1069
40. Chung, C. Y., and Erickson, H. P. (1994) Cell surface annexin II is high affinity receptor for the alternatively spliced segment of tenascin-C. *J. Cell Biol.* **126,** 539–548
41. Fitzpatrick, S. L., Kassam, G., Choi, K. S., Kang, H. M., Fogg, D. K., and Waisman, D. M. (2000) Regulation of plasmin activity by annexin II tetramer. *Biochemistry* **39,** 1021–1028
42. Mai, J., Waisman, D. M., and Sloane, B. F. (2000) Cell surface complex of cathepsin B/annexin II tetramer in malignant progression. *Biochim. Biophys. Acta* **1477,** 215–230
43. Vennekens, R., Hoenderop, J. G., Prenen, J., Stuiver, M., Willems, P. H., Droogmans, G., Nilius, B., and Bindels, R. J. (2000) Permeation and gating properties of the novel epithelial Ca^{2+} channel. *J. Biol. Chem.* **275,** 3963–3969
44. Girard, C., Tinel, N., Terrenoire, C., Romey, G., Lazdunski, M., and Borsotto, M. (2002) p11, an annexin II subunit, an auxiliary protein associated with the background K^+ channel, *TASK-1*. *EMBO J.* **21,** 4439–4448
45. Okuse, K., Malik-Hall, M., Baker, M. D., Poon, W. Y., Kong, H., Chao, M. V., and Wood, J. N. (2002) Annexin II light chain regulates sensory neuronspecific sodium channel expression. *Nature* **417,** 653–656
46. Kirsch, T., Nah, H.-D., Shapiro, I. M., and Pacifici, M. (1997) Regulated production of mineralization-competent matrix vesicles in hypertropic chondrocytes. *J. Cell Biol.* **137,** 1149–1160
47. Kirsch, T., Harrison, G., Golub, E. E., and Nah, H.-D. (2000) The roles of annexins and type II and X collagen in matrix mediated mineralization of growth plate cartilage. *J. Biol. Chem.* **275,** 35577–35583
48. Boros, S., Bindels, R. J., and Hoenderop, J. G. (2009) Active calcium resorption in the connecting tubule. *Pflugers Arch.* **458,** 99–109